Aocgy

A Madden-Julian Oscillation in Tropospheric Ozone

J. R. Ziemke[1, 2] and S. Chandra[1, 2]

[1]University of Maryland Baltimore County (UMBC) Goddard Earth Sciences and Technology (GEST), Baltimore, Maryland

[2]Also at NASA Goddard Space Flight Center, Code 916, Greenbelt, Maryland

Submitted to *Geophysical Research Letters*, August, 2003.

Keywords: Madden-Julian Oscillation, MJO, Intraseasonal Oscillations, Tropospheric Ozone, Tropospheric Water Vapor

Abstract. This is the first study to indicate a Madden-Julian Oscillation (MJO) in tropospheric ozone. Tropospheric ozone is derived using differential measurements of total column ozone and stratospheric column ozone measured from total ozone mapping spectrometer (TOMS) and microwave limb sounder (MLS) instruments. Two broad regions of significant MJO signal are identified in the tropics, one in the western Pacific and the other in the eastern Pacific. Over both regions, MJO variations in tropospheric ozone represent 5-10 Dobson Unit (DU) peak-to-peak anomalies. These variations are significant compared to mean background amounts of 20 DU or less over most of the tropical Pacific. MJO signals of this magnitude would need to be considered when investigating and interpreting particular pollution events since ozone is a precursor of the hydroxyl (OH) radical, the main oxidizing agent of pollutants in the lower atmosphere.

1. Introduction.

The Madden-Julian Oscillation (MJO), also known as a 40-50 day oscillation in winds, temperature, and pressure in the tropical lower atmosphere, was first discovered by *Madden and Julian* [1971]. While many spectral peaks in these signals tend to lie within the 40-50 day band, the MJO shows significant spectral dispersion depending on the state of the background atmosphere, especially changing wind patterns and associated Doppler shifting effects. Because the oscillation may exhibit such spectral variability, many studies have described this phenomenon as "1-2 month oscillations" or more generally as "intraseasonal oscillations". *Madden and Julian* [1971] used several years of surface pressure and tropospheric wind data in the tropics. A more recent paper by *Madden and Julian* [1994] provides an extensive overview of the MJO.

The MJO is associated with large-scale circulation cells in the tropical troposphere and originates primarily over the equatorial Indian Ocean and Pacific Ocean west of the dateline. It is closely associated with enhanced sea-surface temperature anomalies and coupling with ocean dynamics. Along or near the equator the MJO behaves as an eastward propagating Walker circulation cell with wind anomalies being mostly vertical and zonal. The oscillation in temperature and wind is not limited to the equatorial tropics but propagates to middle and high latitudes in the troposphere into both hemispheres with signatures of westward propagating Rossby waves. In summer the oscillation produces an important modulation effect on monsoon, especially in the northern hemisphere. During winter and spring in both hemispheres the MJO propagates not just to high latitudes but also upward into the middle atmosphere (i.e., stratosphere and mesosphere) due to persistent eastward winds at these heights which allow for the vertical propagation of planetary-scale disturbances. The persistence of 40-50 day oscillations in stratospheric ozone and temperature was noted by *Chandra* [1986]. There is also evidence that the MJO propagates even higher into the ionosphere [*Stanford and Saksena*, 1989].

This study examines tropospheric column ozone (TCO) in the tropics from satellite measurements for existence of an MJO signature. An MJO signature in TCO is identified and compared with an MJO signal discovered in a recent study of upper tropospheric humidity (UTH) and 11 μm cloud-top brightness temperature [*Sassi et al.*, 2002].

2. Tropospheric Column Ozone Derived From TOMS and MLS Instruments.

Chandra et al. [2003] describe the TCO data used in this study including details of the algorithm and ozonesonde validation. The data in our investigation are daily maps of TCO with $1^\circ \times 1^\circ$ gridding between latitudes 30°S and 30°N. TCO was determined by subtracting stratospheric column ozone (SCO) from total column ozone. Total column ozone was derived from Nimbus 7 Version 7 total ozone mapping spectrometer (TOMS) measurements. SCO was derived from Upper Atmosphere Research Satellite (UARS) Microwave Limb Sounder (MLS) Version 5 ozone mixing ratio profiles. The TCO data for this study extend from October 1, 1991 through April 30, 1993 when nearly daily measurements were obtained from both TOMS and MLS instruments. The TCO daily data are smoothed using a 5-day running average in time to reduce a known scan bias artifact present in TOMS tropical measurements. The TOMS instrument does not measure ozone lying below optically thick cloud tops and there is a possibility of errors of several DU in total column ozone measurements for these scenes. For this reason we have removed potential cloud-effect problems by removing scenes with reflectivity R greater than 0.2. For investigating the MJO with a 40-50 day timescale, all missing TCO daily data were replaced by linear interpolation first done zonally and then temporally. All other data fields (i.e., SCO, H_2O) incorporated the same interpolation scheme.

3. An MJO Variability in Tropospheric Ozone.

Sassi et al. [2002] identified an MJO signal in MLS UTH and high-altitude "cold-cloud" from Global Cloud Imagery (GCI) data. Their study evaluated data between October 1991 and May 1992 and indicated seven MJO events in these two geophysical parameters near the dateline. In Figure 1 we show a Hovmoller diagram of TCO along the Equator which is compared with Figure 1a of *Sassi et al.* [2002]. Figure 1a of *Sassi et al.* [2002] shows a similar Hovmoller contour plot of 215 hPa MLS UTH and superimposed GCI "cold-cloud" for the same months along the Equator. To be consistent with Figure 1a of *Sassi et al.* [2002], TCO in Figure 1 were further spatially filtered for zonal wavenumbers less than 4 and temporally filtered using a 20-day low-pass digital filter. The seven peak events identified by *Sassi et al.* [2002] are shown as large white numerals in Figure 1. These seven events coincide both temporally and longitudinally with enhanced UTH and cold cloud top (i.e., high cloud) shown in Figure 1a of *Sassi et al.* [2002]. In Figure 1, west of the dateline the period of oscillation is around 40 days. East of the dateline and extending toward the western edge of South America (i.e., around 80°W) there is evidence of an MJO signal but instead with a longer period around 50+ days.

While UTH for these seven events prescribe relative increases, the TCO in Figure 1 indicate decreases. The anti-correlation is consistent with broad-scale convection during MJO events transporting enhanced water vapor into the upper troposphere from below and low boundary-layer ozone causing reduction of TCO. The anti-correlation between TCO and upper-level H_2O was described in an earlier study by *Chandra et al.* [1998] which compared relationships between TCO and H_2O on interannual timescales. It is noted that the reduction in TCO associated with convection has been described in several investigations including recent observation/modeling studies by *Sudo and Takahashi* [2001] and *Chandra et al.* [2002].

For the time period October 1, 1991 through May 30, 1992 (244 days), the largest MJO signal-to-noise in TCO appears to lie within latitudes ±20° over two large regions in the eastern and western Pacific (Figure 2). Estimates of MJO signal (spectral power) for this time period were evaluated by first applying a Hanning window to each time series followed by Fourier analysis. Hanning was applied to limit spectral leakage effects to only nearest-neighbor Fourier coefficients. A 3-point running average was applied to the power periodogram as a spectral estimator. Background noise was estimated by applying a first-order autoregressive (i.e., Markov) noise model to the Hanned time series.

Statistical significance testing was applied to signals lying in the 35-60 day band. Signal-to-noise power ratios exceeding 2.1 in this window are significant at the 95% confidence level.

4. Time Series in the Pacific.

Time series of TCO and MLS 215 hPa H_2O volume mixing ratio are shown in Figure 3, which includes comparison with SCO. The chosen location (Equator, 150°E) lies within the broad region of statistical significance for an MJO signal in the western Pacific (see Figure 2). For better visualization of MJO signals a 20-day lowpass filter was applied to both daily H_2O and TCO timeseries. The H_2O data are MLS volume mixing ratio used previously by *Chandra et al.* [1998] and discussed in detail by *Read et al.* [1995, 2001]. As in *Chandra et al.* [1998], Figure 3 shows an anti-correlation between H_2O and TCO but on a much shorter time scale (1-2 months) over the entire period shown. (For completeness, time series comparisons were extended to include all available data for the Nimbus 7 time period, October 1991-April 1993.) Peak-to-peak anomalies in TCO are around 5-10 DU and are sizable compared to mean background amounts which are around 20 DU or less. The third curve in Figure 2 is SCO which does not indicate an apparent MJO signal. It has been demonstrated in early studies using either satellite observations [e.g., *Gao and Stanford*, 1987] or modeling [e.g., *Garcia and Salby*, 1987] that there is little vertical propagation of MJO disturbances into the stratosphere in tropical latitudes. With this constraint on the oscillation, total column ozone should indicate the same peak-to-peak anomalies. Evidence for MJO variability in total column ozone was first shown by *Sabutis et al.* [1987] using TOMS measurements.

Figure 4 shows a similar time series comparison of TCO and H_2O in the western Pacific, but located further north and further east at 10°N and 165°E. This location also lies within the same general region of statistical significance in the western Pacific (see Figure 2). As in Figure 3, there is an indication of a general anti-correlation between TCO and H_2O on MJO timescale over the entire time period, and suggests a modulation of convective transport as a source for these constituent anomalies. Figure 5 shows another line plot comparing TCO and H_2O but instead at 10°S and 135°W, near the center of detected MJO signal in the southeastern Pacific (see Figure 2). There is again a general indication of an anti-correlation between TCO and H_2O on an MJO timescale during the first half of the record, and an additional anticorrelation but on a longer timescale after July 1992. The drop in H_2O and rapid increase in TCO after July 1992 suggests a substantial reduction in convection on a seasonal timescale. On an MJO timescale, peak-to-peak anomalies in TCO in Figures 4-5 are around 5-10 DU. It is noted that observational evidence for an MJO signal in the southeastern Pacific was first shown by *Gao and Stanford* [1987] from Microwave Sounding Unit (MSU) satellite temperature measurements and by *Graves and Stanford* [1987] using rawinsonde measurements from Easter Island (27°S, 109°W).

5. Conclusions.

In this paper we provide the first evidence of a Madden-Julian Oscillation in tropospheric ozone. TCO derived from TOMS/MLS measurements was compared with upper tropospheric H_2O from UARS MLS. A general anti-correlation with upper tropospheric H_2O on an MJO timescale suggests convection as a source for these oscillations. For the time period October 1991 through May 1992, a sequence of several distinct MJO events were observed in the tropics. Two large regions were identified for MJO signals in TCO. One region is in the western Pacific extending from the Equator to 20°N and the other in the eastern Pacific extending from the Equator to 20°S. MJO variability in TCO exhibits around 5-10 DU peak-to-peak anomalies in the regions. These changes in TCO are large, especially when compared to background TCO amounts of around 20 DU or less in the Pacific.

The MJO may thus have a significant role in regulating the chemical cycles associated with the change in tropospheric ozone. As noted by *Kley et al.* [1996], ozone is the main precursor molecule for hydroxyl (OH) radicals, the primary oxidizing agent in the atmosphere. A decrease in ozone and OH will result in the reduction of chemical removal rates of gases that are released to the atmosphere from the ocean. The models, therefore, should account for MJO as it introduces sizable variations in TCO at 5-10 DU. It is interesting to note that a large decrease in tropospheric ozone in the equatorial Pacific during March 1993 reported by *Kley et al.* [1996] may be a manifestation of the MJO since it coincides with a trough in the MJO cycle as indicated in Figure 3.

Acknowledgments. We wish to thank William G. Read for providing the MLS tropospheric H_2O data used in this study.

References.

Chandra, S., The solar and dynamically induced oscillations in the stratosphere, *J. Geophys. Res., 91,* 2719-2734, 1986.

Chandra, S., J. R. Ziemke, W. Min, and W. G. Read, Effects of 1997-1998 El Nino on tropospheric ozone and water vapor, *Geophys. Res. Lett., 25*, 3867-3870, 1998.

Chandra, S., J. R. Ziemke, P. K. Bhartia, and R. V. Martin, Tropical tropospheric ozone: Implications for dynamics and biomass burning, *J. Geophys. Res., 107* (D14), 10.1029/2001JD000447, 2002.

Chandra, S., J. R. Ziemke, and R. V. Martin, Tropospheric ozone at tropical and middle latitudes derived from TOMS/MLS residual: Comparison with a global model, *J. Geophys. Res., 108* (D9), 10.1029/2002JD002912, 2003.

Gao, X. H., and J. L. Stanford, Low-frequency oscillations of the large-scale stratospheric temperature field, *J. Atmos. Sci.*, 44, 1991-2000, 1987.

Garcia, R. R., and M. L. Salby, Transient response to localized episodic heating in the tropics. Part II: Far-field behavior, *J. Atmos. Sci., 44*, 499-530, 1987.

Graves, C. E., and J. L. Stanford, Low-frequency atmospheric oscillations over the southeastern Pacific, *J. Atmos. Sci., 44*, 260-264, 1987.

Kley, et al., Observations of near-zero ozone concentrations over the convective Pacific: Effects on air chemistry, *Science, 274*, 230-232, 1996.

Madden, R. A., and P. R. Julian, Detection of a 40-50 day oscillation in the zonal wind in the tropical Pacific, *J. Atmos. Sci., 28*, 702-708, 1971.

Madden, R. A., and P. R. Julian, Observations of the 40-50 Day Tropical Oscillation – A review, *Mon. Wea. Rev., 122*, 814-837, 1994.

Read, W. G., J. Waters, D. A. Flower, L. Froidevaux, R. F. Jarnot, D. L. Hartmann, R. S. Harwood, and R. B. Rood, Upper tropospheric water vapor from UARS MLS, *Bull. Am. Meteorol. Soc., 76*, 2381-2389, 1995.

Read, W. G., et al., UARS Microwave Limb Sounder upper tropospheric humidity measurement: Method and validation, *J. Geophys. Res., 106*, 32,207-32,258, 2001.

Sabutis, J. L., J. L. Stanford, and K. P. Bowman, Evidence for 35-50 day low-frequency oscillations in total ozone mapping spectrometer data, *Geophys. Res. Lett., 14*, 945-947, 1987.

Sassi, F., M. Salby, H. C. Pumphrey, and W. G. Read, Influence of the Madden-Julian

Oscillation on upper tropospheric humidity, *J. Geophys. Res., 107* (D23), 10.1029/2001JD001331, 2002.

Stanford, J. L., and R. C. Saksena, Oscillations in D-region absorption at periods of one to two months, *J. Atmos. Terr. Phys., 51*, 955-981, 1989.

Sudo, K., and M. Takahashi, Simulation of tropospheric ozone changes during 1997-1998 El Nino: Meteorological impact on tropospheric photochemistry, *Geophys. Res. Lett., 28*, 4091-4094, 2001.

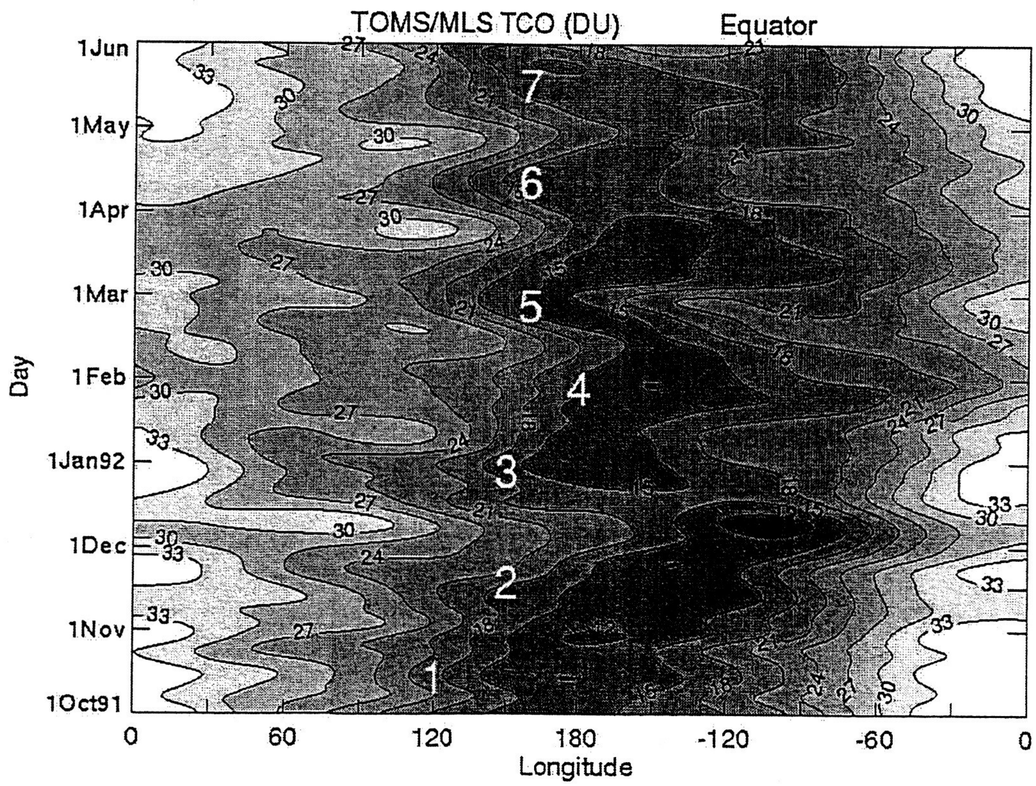

Figure 1. Day versus longitude Hovmoller diagram of TCO (in DU) along the Equator for October 1, 1991 through May 30, 1992. The TCO data were temporally low-pass filtered (half-amplitude filter response at 20-day period) and spatially filtered for zonal wavenumbers 0-3.

TCO MJO Signal-To-Noise Ratio Test 95% Confidence Level

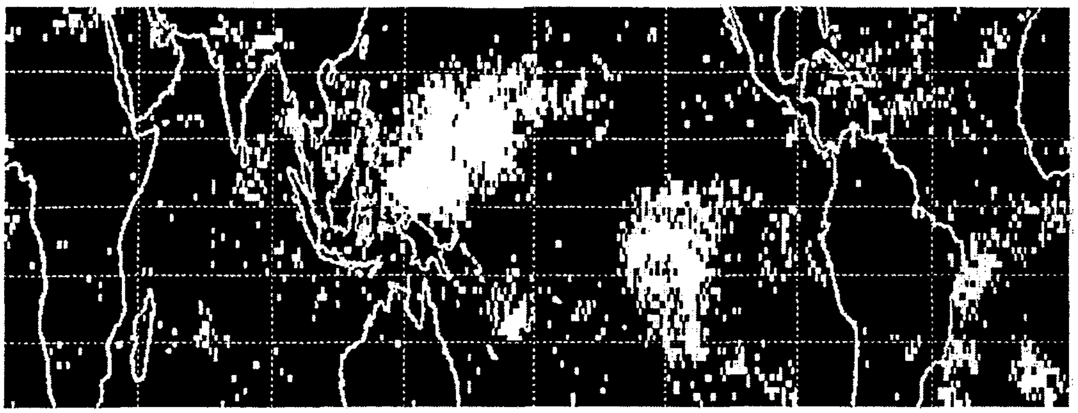

Figure 2. Grid points with an MJO signal in TCO at the 95% confidence level. Grid points which pass 95% confidence (signal-to-noise power ratio greater than 2.1) are white. (See section 3 for discussion of signal-to-noise calculation). Latitude gridlines extend from 30°S to 30°N with 10° increment. Longitude gridlines (45° increment) extend completely around the earth beginning at furthest left at longitude 0°.

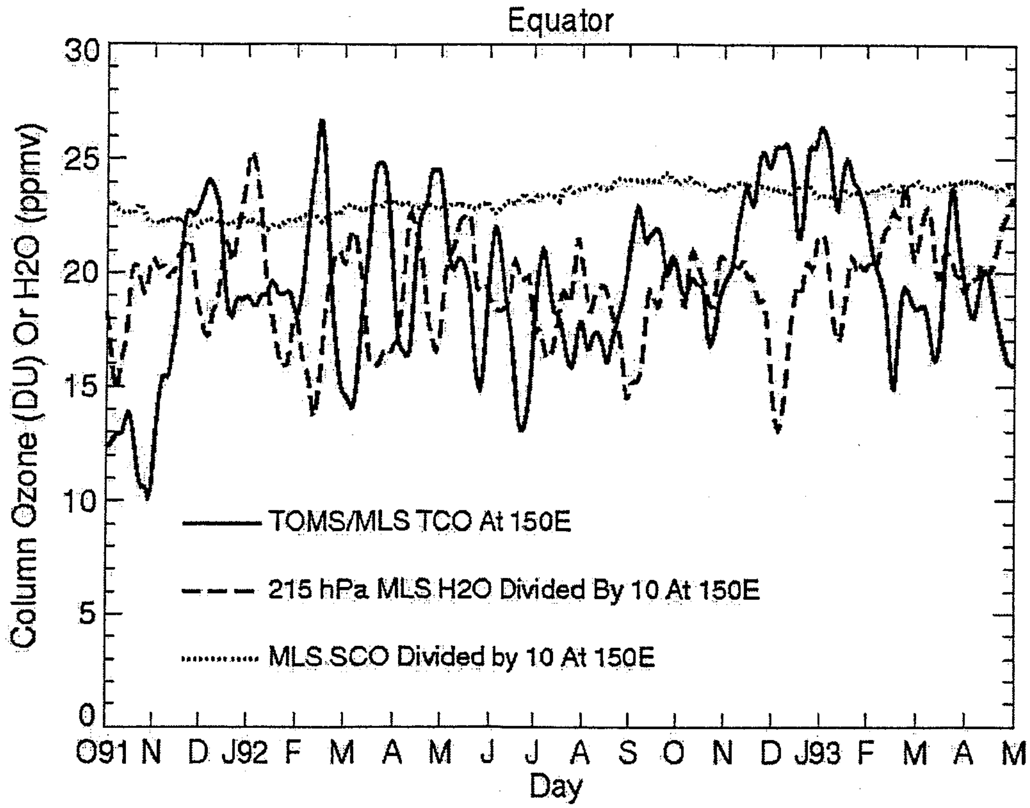

Figure 3. Daily time series of TCO (solid), 215 hPa H_2O (dashed), and SCO (dotted) along the Equator at longitude 150°E. Vertical units are either ppmv or DU (indicated). Time period plotted: October 1, 1991 through April 30, 1993. A 20-day low-pass filter was applied to both TCO and H_2O time series. SCO are daily measurements with no additional filtering.

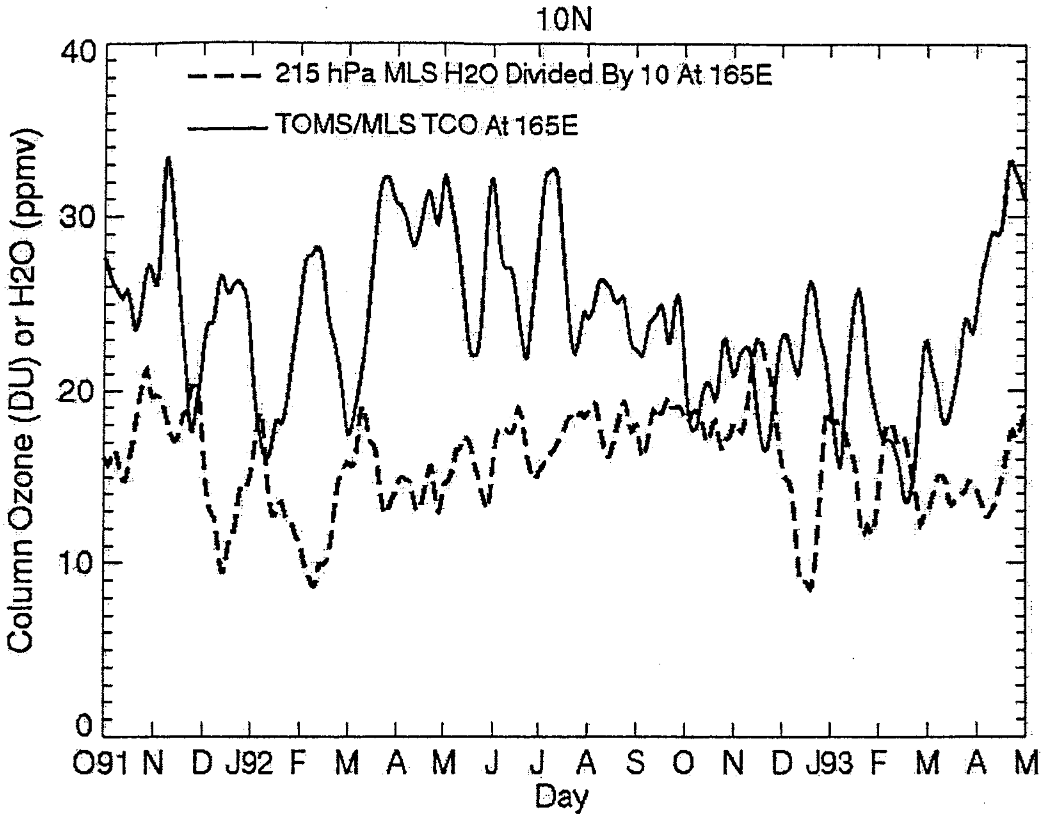

Figure 4. Same as Figure 3 but without SCO and with a different western Pacific grid point: 10°N, 165°E.

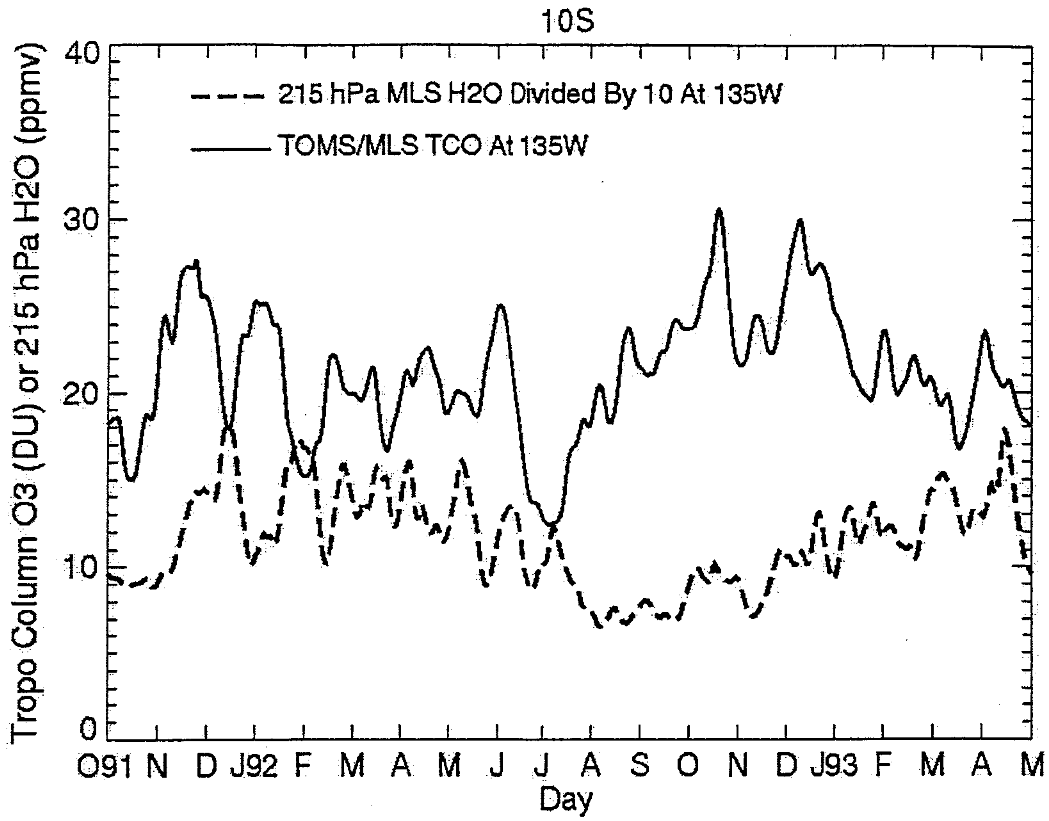

Figure 5. Same as Figure 3 but without SCO and with a different grid point in the eastern Pacific: 10°S, 135°W.